Effects of salinity on glycerol conversion and biological phosphorus removal by aerobic granular sludge

Elahinik, Ali; de Clercq, Fleur; Pabst, Martin; Xevgenos, Dimitrios; van Loosdrecht, Mark C.M.; Pronk, Mario

DOI
10.1016/j.watres.2024.121737

Publication date
2024

Document Version
Final published version

Published in
Water Research

Citation (APA)
Elahinik, A., de Clercq, F., Pabst, M., Xevgenos, D., van Loosdrecht, M. C. M., & Pronk, M. (2024). Effects of salinity on glycerol conversion and biological phosphorus removal by aerobic granular sludge. *Water Research*, *257*, Article 121737. https://doi.org/10.1016/j.watres.2024.121737

Water Research 257 (2024) 121737

Contents lists available at ScienceDirect

Water Research

journal homepage: www.elsevier.com/locate/watres

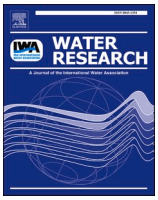

Effects of salinity on glycerol conversion and biological phosphorus removal by aerobic granular sludge

Ali Elahinik [a,*], Fleur de Clercq [a], Martin Pabst [a], Dimitrios Xevgenos [b], Mark C.M. van Loosdrecht [a], Mario Pronk [a,c]

[a] Department of Biotechnology, Delft University of Technology, van der Maasweg 9 2629HZ, Delft, The Netherlands
[b] Department of Technology, Policy, and Management, Delft University of Technology, van der Jaffalaan 5 2628 BX, Delft, The Netherlands
[c] Royal HaskoningDHV, Laan 1914 no 35 3800AL, Amersfoort, The Netherlands

ARTICLE INFO

Keywords:
Aerobic granular sludge
EBPR
Glycerol
Salinity
Trehalose
Metaproteomics

ABSTRACT

Industrial wastewater often has high levels of salt, either due to seawater or e.g. sodium chloride (NaCl) usage in the processing. Previous work indicated that aerobic granular sludge (AGS) is differently affected by seawater or saline water at similar osmotic strength. Here we investigate in more detail the impact of NaCl concentrations and seawater on the granulation and conversion processes for AGS wastewater treatment. Glycerol was used as the carbon source since it is regularly present in industrial wastewaters, and to allow the evaluation of microbial interactions that better reflect real conditions. Long-term experiments were performed to evaluate and compare the effect of salinity on granulation, anaerobic conversions, phosphate removal, and the microbial community. Smooth and stable granules as well as enhanced biological phosphorus removal (EBPR) were achieved up to 20 g/L NaCl or when using seawater. However, at NaCl levels comparable to seawater strength (30 g/L) incomplete anaerobic glycerol uptake and aerobic phosphate uptake were observed, the effluent turbidity increased, and filamentous granules began to appear. The latter is likely due to the direct aerobic growth on the leftover substrate after the anaerobic feeding period. In all reactor conditions, except the reactor with 30 g/L NaCl, *Ca.* Accumulibacter was the dominant microorganism. In the reactor with 30 g/L NaCl, the relative abundance of *Ca.* Accumulibacter decreased to $\leq$1 % and an increase in the genus *Zoogloea* was observed. Throughout all reactor conditions, *Tessaracoccus* and *Micropruina*, both actinobacteria, were present which were likely responsible for the anaerobic conversion of glycerol into volatile fatty acids. None of the glycerol metabolizing proteins were detected in *Ca.* Accumulibacter which supports previous findings that glycerol can not be directly utilized by *Ca.* Accumulibacter. The proteome profile of the dominant taxa was analysed and the results are further discussed. The exposure of salt-adapted biomass to hypo-osmotic conditions led to significant trehalose and PO_4^{3-}-P release which can be related to the osmoregulation of the cells. Overall, this study provides insights into the effect of salt on the operation and stability of the EBPR and AGS processes. The findings suggest that maintaining a balanced cation ratio is likely to be more important for the operational stability of EBPR and AGS systems than absolute salt concentrations.

1. Introduction

Many wastewaters of industrial origin, such as epoxy resin production or food processing facilities, contain high concentrations (>1 % wt) of sodium chloride (NaCl), which are often accompanied by high organic content (>1000 mg/L chemical oxygen demand (COD) (Lefebvre and Moletta, 2006; Madigan et al., 2000; Pronk et al., 2014; Sanna et al., 1991). In line with the objectives of circular economy solutions for industrial brines, compounds such as NaCl present in industrial brines can be recovered by applying suitable brine treatment technologies able to capture the circular water value of brine effluent streams (Xevgenos et al., 2024). The reuse of salt entails the removal of organics to achieve high-purity brine to be used in other applications such as the chlor-alkali process. Utilizing reverse osmosis for NaCl recycling similarly demands high-purity brine, as the presence of organics can severely decrease the efficiency of these systems. Moreover, municipal wastewater with

* Corresponding author.
E-mail address: a.elahinik@tudelft.nl (A. Elahinik).

https://doi.org/10.1016/j.watres.2024.121737
Received 7 March 2024; Received in revised form 1 May 2024; Accepted 3 May 2024
Available online 4 May 2024

seawater flushing or intrusion also contains high salinity that must be treated before discharge (EU Water Framework Directive, 2000).

To remove organics, aerobic granular sludge (AGS) can be applied as a biological wastewater treatment technology. AGS is a highly efficient method of treating wastewater, offering numerous benefits over traditional activated sludge systems (Bengtsson et al., 2018; de Bruin et al., 2004; Pronk et al., 2015). The granular structure of the biofilm allows for fast settling and the substrate and oxygen gradient across the granules enables simultaneous conversions to take place, leading to a reduced treatment time and improved solid-liquid separation (Bassin et al., 2012). The formation of aerobic granules was first reported in the late 1990s (Beun et al., 1999; Heijnen and Van Loosdrecht, 1998; Morgenroth et al., 1997), and has since been the subject of extensive research to better understand the mechanisms behind their formation and stability (Haaksman et al., 2023; van Dijk et al., 2022). During substrate feeding under anaerobic conditions, polyhydroxyalkanoates (PHA) are stored and later utilized by slow-growing heterotrophs in the subsequent aerobic phase. This leads to the formation of compact granular biofilms by preventing transfer-limited growth (de Kreuk and van Loosdrecht, 2004).

Salt can negatively affect wastewater processes including AGS processes. For example, by altering the microbial community composition and anaerobic-aerobic conversions which can influence the effluent quality and solid-liquid separation due to the proliferation of filamentous organisms and destabilization of the biofilm matrix (Bassin et al., 2011; Pronk et al., 2014; Sivasubramanian et al., 2021; Welles et al., 2014). There are indications that salt water with mainly NaCl will have a different impact than seawater salinity (de Graaff et al., 2020a). In this study, the aim was to evaluate this difference in more detail. All studies describing some effects of salt have been performed with acetate as the carbon source (Bassin et al., 2011; de Graaff et al., 2020b; Figueroa et al., 2008; Pronk et al., 2014; X. Wang et al., 2017). Here, we chose to use glycerol, a sugar alcohol, as the carbon substrate. The use of sugars such as glycerol promotes a more diverse microbial community compared to VFAs (Elahinik et al., 2022), which allows for studying the microbial interactions in such systems. Fermentative microorganisms convert sugars into fermentation products, that can be utilized by e.g. phosphate-accumulating and glycogen-accumulating microorganisms. This creates a microbial cross-feeding relationship, where different species depend on each other for the breakdown and utilization of substrates, fostering diversity (Elahinik et al., 2022;2023). From the application point of view, glycerol is also a compound found in many industrial waste streams such as the epoxy and biodiesel production facilities, which makes it an interesting substrate to study concerning the AGS processes.

The enhanced biological phosphorus removal (EBPR) process is an energy-efficient and cost-effective technology (Barnard, 1975). This technology is centred on the enrichment of the sludge with phosphorus-accumulating organisms (PAO) that can accumulate excessive amounts of phosphorus (P) in the form of poly-phosphate (poly-P). The removal of phosphorus is then achieved by discharging the excess sludge containing accumulated phosphorus (Smolders et al., 1995). Given the similarity in operational parameters between the EBPR and AGS processes, they can be studied concurrently.

This study aims to investigate the effects of varying concentrations of NaCl (10–30 g/L) in comparison to synthetic seawater (35 g/L) on granulation and EBPR process using glycerol as the sole carbon source. Detailed information on the kinetic and anaerobic-aerobic conversions, the main bacterial species involved, the changes in the microbial community, and the granulation of the AGS system performing EBPR is provided. The study also evaluates the enzymatic machinery of the dominant taxa and the key processes such as osmoregulation, substrate storage, and fermentation under saline conditions via metaproteomics.

2. Material and methods

2.1. Experimental setup and reactor operation

A bubble column reactor with a working volume of 3.1 L, an internal diameter of 5.6 cm, and a total height of 90 cm was operated in sequencing batch reactor (SBR) mode. After 1.5 L effluent withdrawal at the end of each cycle, a volumetric exchange ratio of 48 % was maintained. The pH was controlled at 7.1 ± 0.1 by automatic dosing of 0.5 M NaOH or HCl. The dissolved oxygen (DO) concentration was controlled at 0 % and 50 % (3.5 mg/L) saturation during the anaerobic and aerobic phase, respectively, by a mixture of nitrogen gas and air. The off-gas was recirculated with a flow of 5 L/min to maintain the DO concentration. The DO probes were calibrated for each salt concentration. The temperature of the reactor was not directly controlled but the room temperature was controlled at 20 °C. The reactor was inoculated with ≈ 600 mL of a mixture of aerobic granular sludge from a pilot-scale municipal wastewater treatment reactor performing EBPR located in Harnaschpolder, the Netherlands and glycerol-adapted sludge performing EBPR from previous experiments. Each cycle consisted of 5 min of nitrogen sparging to ensure anaerobic condition before feeding followed by 5 min of feeding, 60 min of nitrogen sparging (anaerobic phase), 120 min of aeration (aerobic phase), 5 min of settling, and 5 min of effluent withdrawal.

The synthetic influent fed at the beginning of each cycle with a total volume of 1500 mL consisted of 1200 mL of salt water (10 – 30 g/L NaCl or 35 g/L synthetic sea salt), 150 mL of nutrient medium and 150 mL of carbon medium. Synthetic seawater with a final concentration of 35 g/L was made with Instant Ocean® sea salt (Atkinson et al., 1997). 35 g/L sea salt was used to account for the mass of other elements in the mixture and to achieve a 30 g/L NaCl equivalent. All other reactor operational conditions were kept constant, except the aforementioned salinity. Carbon medium contained 35.7 mM glycerol, 3.6 mM $MgSO_4{\cdot}7H_2O$, and 4.7 mM KCl. The nutrient medium contained 41.1 mM NH_4Cl, 1.95 mM K_2HPO_4, 1.98 mM KH_2PO_4, 0.6 mM Allythiourea (ATU) to inhibit nitrification and 10 mL/L of trace element solution. The trace element solution contained 4.99 g/L $FeSO_4{\cdot}7H_2O$, 2.2 g/L $Zn.SO_4{\cdot}7H_2O$, 7.33 g/L $CaCl_2{\cdot}2H_2O$, 4.32 g/L $MnSO_4.H_2O$, 2.18 g/L $Na_2MoO_4{\cdot}2H_2O$, 1.57 g/L $CuSO_4{\cdot}5H_2O$, 1.61 g/L $CoCl_2{\cdot}6H_2O$ and 50 g/L EDTA. The combination of these feed sources resulted in a final influent concentration of 400 mg/L COD, 58 mg/L NH_4^+-N, and 12 mg/L of PO_4^{3-}-P. The ratio of major cations relative to sodium in seawater, synthetic seawater (I.O.), and medium dosed with pure NaCl with different concentrations is presented in Table 1.

Batch experiments were performed in 250 mL bottles with glycerol- and propionate-adapted sludge performing phosphate removal to evaluate whether glycerol can be directly taken up under anaerobic conditions. The bottle was sparged with nitrogen to ensure an anaerobic environment and controlled pH at 7 ± 0.1 by manual dosing of 0.5 M HCl or NaOH. The propionate-adapted biomass was selected as a control from an existing reactor. Biomass at the end of the aerobic phase (end of

Table 1
The ratio of magnesium and potassium relative to sodium in seawater, synthetic sea salt (I.O.), and medium dosed with pure NaCl with different concentrations. The absolute concentrations of the respective elements are shown. The elemental composition of seawater and I.O. is given in (Atkinson et al., 1997).

Parameters	Seawater	I.O.	30 g/L NaCl	20 g/L NaCl	10 g/L NaCl
Na^+/Mg^{2+}	8	8	1346	897	449
Na^+/K^+	27	29	643	429	214
Na^+ [g]	16	16	18	12	6
K^+ [mg]	598	551	28	28	28
Mg^{2+} [mg]	1932	1895	13	13	13
Osmolarity [atm]	27	26	26	21	17

the cycle) was taken from the reactor and used as inoculum (20 mL).

2.2. Analytical methods

Concentrations of PO_4^{3-}-P and NH_4^+-N were measured using a Gallery Discrete Analyser (ThermoFisher Scientific, USA). Chemical oxygen demand was measured with a spectrophotometer cuvette system (DR2800, Hach Lange, USA). Volatile fatty acids and sugars were measured using an HPLC (Vanquish, ThermoFisher Scientific, USA) equipped with an RI and UV detector, Aminex HPX-87H column (Bio-Rad, USA) using 0.0015 M phosphoric acid as eluent.

2.3. PHA & glycogen determination

Biomass samples from the reactor were fixed with 4% w/v para-formaldehyde, washed with demineralized water, freeze-dried overnight and crushed into fine powder. For extraction, approximately 30 mg of the powered biomass was hydrolysed and esterified in a 10 % sulphuric acid, methanol, and chloroform solution for 24 h at 100 °C with frequent manual vortex. For phase separation, 3 mL of ultrapure water was added to the samples and the formed esters in the organic phase were then filtered and analysed by a GC (6890 N, Agilent, USA). Quantifications of PHB, PHV, and PH2MV were done using commercial 3-hydroxybutyrate, a synthetic copolymer of (*R*)-3-hydroxybutyrate-(*R*)-3-hydroxyvalerate (Sigma-Aldrich, USA), and 3-Hydroxy-2-methyl-valeric acid (BenChem, USA), respectively. Benzoic acid was also added to the samples as an internal standard.

2.4. Microscopy

To observe and capture the morphology of the granules, a stereo zoom microscope (M205 FA, Leica Microsystems, Germany) equipped with Qwin image analysis software (V3.5.1, Leica Microsystems, Germany) was used. The phase contrast pictures of the microbial population were taken with Axio Imager M2 (Zeiss, Germany).

2.5. Metagenomics and metaproteomics

The DNA from the biomass samples was extracted using the DNeasy PowerSoil Pro-Kit (Qiagen, Germany) following the manufacturer's protocol. Metagenome sequencing and raw data processing were conducted by Novogene (Novogene Co., China). For protein extraction and metaproteome analysis, the methodology described by Kleikamp et al. (2022) was followed. Similar to (Elahinik et al., 2022), the functional proteins were annotated using the KEGG database, and the metaproteome raw data was analysed using the metagenome-constructed dataset.

3. Results

3.1. Reactor operation

A bubble column reactor with aerobic granular sludge was operated in sequencing batch mode for over 300 days. The reactor was operated in four different conditions each characterized by varying salinity (Table 1). About 50 mL of crushed granular sludge from a full-scale WWTP located in Harnaschpolder, the Netherlands was used to supplement the biomass in the reactor at the beginning of each condition to ensure proper microbial diversity. The concentrations of orthophosphate and readily biodegradable COD (rbCOD) measured over time are shown in Fig. 1. The rbCOD represents glycerol and potential products formed in the bulk liquid at the end of the anaerobic phase. The conversion of glycerol in an AGS system under fresh-water conditions was previously studied (Elahinik et al., 2022) where the anaerobic reactions seemed to be a combination of glycerol conversion (to mainly propionate) by the fermentative community and product uptake-type reaction

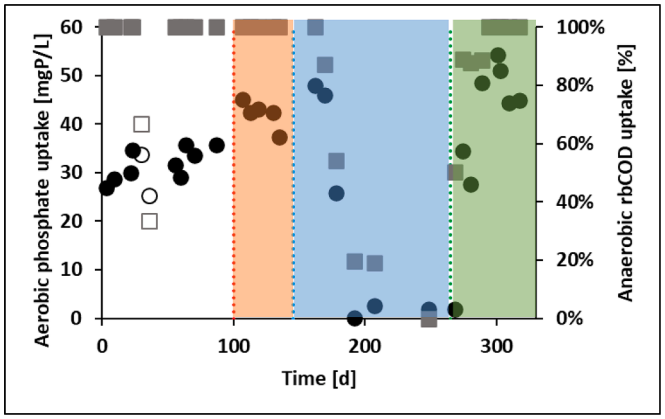

Fig. 1. Concentrations of orthophosphate (circles) and percentage of rbCOD consumed (squares) at the end of the anaerobic phase over time. rbCOD represents glycerol and potential products formed in the anaerobic phase. Hollow markers show operational failure due to technical issues. The shaded areas indicate the switch from 10 to 20 g/L NaCl (red), 20 to 30 g/L NaCl (blue), and from 30 g/L NaCl to 35 g/L sea salt (green).

by the PAOs. At 10 and 20 g/L NaCl complete anaerobic glycerol uptake as well as phosphate release and uptake was observed, similar to fresh-water conditions. At 30 g/L NaCl, glycerol was only partly converted into propionate in the anaerobic phase and propionate accumulation in the liquid phase was observed (Fig. 4). Leftover glycerol and propionate were oxidized in the subsequent aerobic phase. This resulted in reduced anaerobic phosphate release and aerobic uptake until complete EBPR deterioration. In seawater conditions (switching to 35 g/L sea salt), anaerobic glycerol uptake increased and phosphate release was observed (Fig. 1). Average specific phosphate and ammonium conversions at each salt concentration are presented in Table 2. Ammonium consumption is due to biomass growth since ATU was added to inhibit nitrification.

At 30 g/L NaCl, incomplete anaerobic substrate uptake led to aerobic conversion of the carbon source and some filamentous growth was observed (Fig. 2.C&D). With increasing NaCl concentration, the effluent suspended solids concentration increased threefold (Table 3) as can also be seen in the murky background (Fig. 2.D). Microscopic analysis of the effluent showed the presence of suspended cell aggregates and staining of effluent suspended solids with Alcian blue, showed the presence of cells entrapped in extracellular acidic polysaccharides (Fig. 2.F). By switching the salt from 30 g/L NaCl to 35 g/L sea salt, the effluent turbidity decreased and the formation of new granular biomass and a compact settled bed was observed. The average dry weight measurements, solid retention time (SRT), and sludge volume index (SVI_5) are presented in Table 3.

The SRT was controlled between 12 - 17 days through a combination of manual sludge removal and solids washout with the effluent. At 20 and 30 g/L NaCl, manual sludge removal was reduced to preserve a sufficient amount of biomass within the reactor, resulting in an increase in the SRT (Table 3). This was done to increase substrate utilization and offset potential disturbances due to higher salinity. The VSS/TSS ratio at 10 and 20 g/L NaCl enrichment were 0.72 & 0.73, respectively, and are comparable to freshwater enrichments with glycerol with a ratio of 0.75. However, the ratio increased to 0.89 as the NaCl concentration increased to 30 g/L. At 35 g/L sea salt, with the restoration of EBPR activity, the VSS/TSS ratio dropped to 0.75.

3.2. Batch tests

Batch tests were performed with glycerol- and propionate-adapted sludge enriched with PAOs to evaluate whether glycerol can be directly taken up under anaerobic conditions by PAOs. We chose

Table 2
Average specific phosphate and ammonium conversions during reactor pseudo-steady-state operation. Standard deviations are included. * Values from the freshwater conditions are retrieved from (Elahinik et al., 2022) and are provided as a reference.

Salt	Freshwater*	NaCl 10	NaCl 20	NaCl 30	Sea salt 35	g/L
P-release	11.21 ± 1.0	3.54 ± 0.9	5.10 ± 1.1	0.10 ± 0.1	3.84 ± 0.8	*mgP/gVSS*
P-uptake	8.09 ± 0.8	4.17 ± 1.0	5.89 ± 1.1	0.24 ± 0.2	4.35 ± 0.8	*mgP/gVSS*
N-consumption	1.42 ± 0.1	1.02 ± 0.4	1.30 ± 0.2	1.02 ± 0.2	0.78 ± 0.2	*mgN/gVSS*

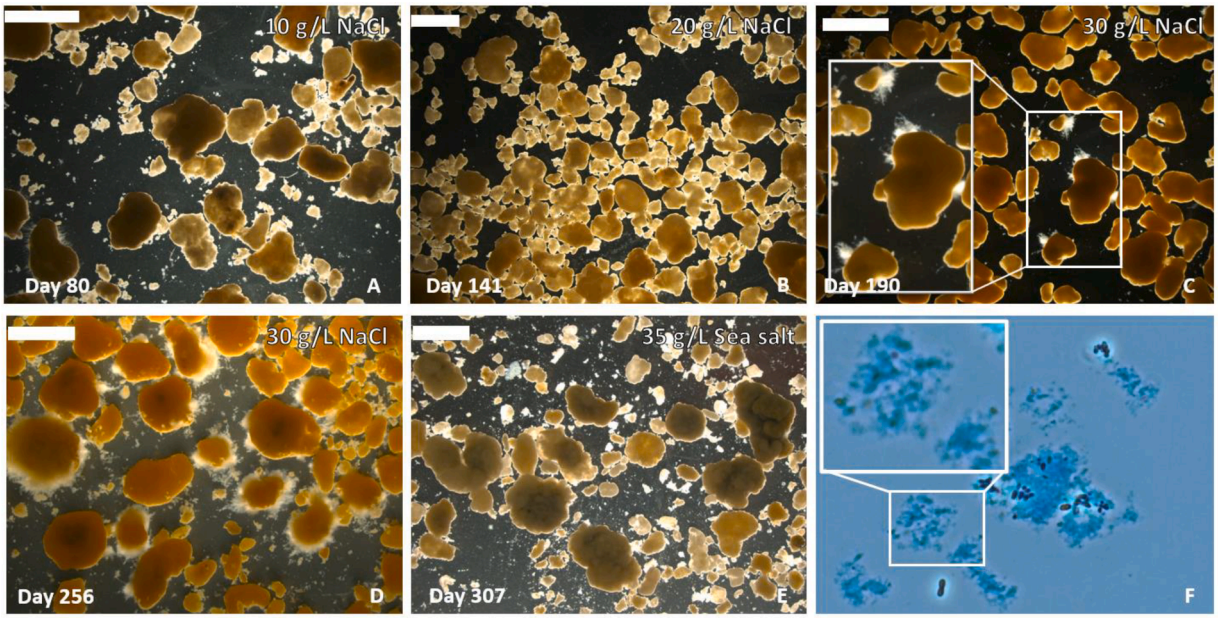

Fig. 2. Stereoscopic image of steady-state aerobic granular sludge cultivated at the end of each salinity. The days when the pictures were taken are indicated (see Fig. 1 for reference). Pictures (A) and (B) show the granules at 10 and 20 g/L NaCl, respectively. Pictures (C) and (D) show the appearance and proliferation of filamentous granules at 30 g/L NaCl, respectively. Picture (E) shows the granules at 35 g/L sea salt. Picture (F) shows Alcian blue staining of the effluent suspended solids. Scale bar equals 3 mm (A-D) and 1 mm (E).

Table 3
Average dry weight measurements, SRT, and SVI_5 for each respective salt concentration are shown. Standard deviations are also provided. * Values from the freshwater conditions are retrieved from (Elahinik et al., 2022) and are provided as a reference.

Parameters	**Values**					**Units**
Salt	Freshwater*	NaCl 10	NaCl 20	NaCl 30	Sea salt 35	*g/L*
SRT	12	12	17	17	12	*d*
SVI_5	33.4 ± 1.9	15.4 ± 3.3	16.7 ± 1.7	18.1 ± 2.6	9.8 ± 2.2	*mL/g*
TSS	7.3 ± 0.5	13.1 ± 0.5	10.2 ± 1.1	8.8 ± 1.9	15.3 ± 2.2	*g/L*
VSS	5.5 ± 0.3	9.5 ± 0.5	7.4 ± 0.8	7.8 ± 1.8	11.47 ±1.6	*g/L*
VSS/TSS	0.75±0.02	0.73 ±0.02	0.72 ±0.00	0.89 ±0.02	0.75 ±0.01	*g/g*
Effluent TSS	0.07±0.02	0.12 ±0.01	0.19 ±0.09	0.30 ±0.16	0.10 ±0.02	*g/L*

biomass from an existing reactor in the lab that was fed with propionate only as a control. More information about the seed sludge used in the batch tests can be found in Elahinik et al. (2022). This test aimed to verify the findings of a recent study (Elahinik et al., 2022) which suggested that glycerol conversion in AGS-EBPR systems was a combination of substrate fermentation by fermentative organisms and product uptake reaction by PAOs. As shown in Fig. 3, the results revealed that the propionate-adapted biomass was not able to utilize glycerol directly as expected. Nonetheless, both systems displayed a comparable trend in

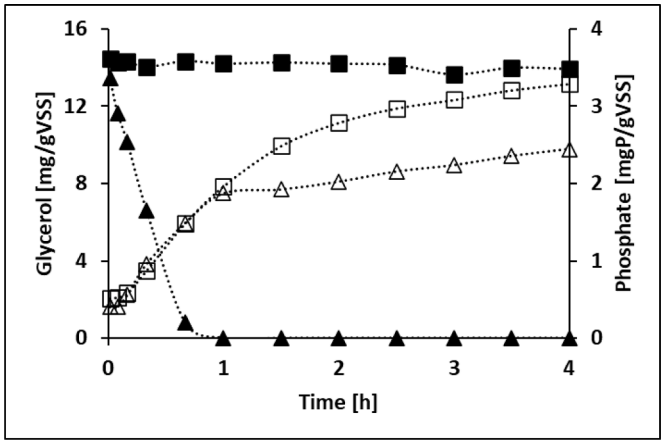

Fig. 3. Glycerol (solid markers) and phosphate (hollow markers) concentrations under anaerobic conditions by glycerol enrichment (triangles) and propionate enrichment (squares).

primary phosphorus release with a rate of 2.9 mgP/gVSS/h. This finding prompted us to investigate if glycerol induced an osmotic stress on the propionate-enrichment, which could cause P-release. To address this concern, we conducted a separate test (data not shown) with and without glycerol in the medium but found that the P-release profile was similar. This indicated that P-release occurs regardless of the presence of glycerol in the glycerol-adapted biomass.

3.3. Typical cycle behaviour

Fig. 4. shows the behaviour of a typical cycle for each salinity tested during reactor pseudo-steady-state operation. From this, the rates and stoichiometries are obtained and listed in Table 4. The pseudo-steady-state was defined based on stable glycerol and phosphate conversions for more than at least 1 SRT. In the anaerobic phase, glycerol uptake, P-release and PHA accumulation were observed at 10 and 20 g/L NaCl. In the subsequent aerobic phase, P-uptake and PHA oxidation occurred. The only storage polymer detected was PHV. No PHB or PH2MV was detected. Due to the potential occurrence of simultaneous glycogen degradation and accumulation, and trehalose presence, the anaerobic glycogen hydrolysis was estimated based on the type and the amount of PHA produced as described by (Elahinik et al., 2022). Mass balances were performed over anaerobic glycerol uptake, PHV accumulation and theoretical glycogen hydrolysis. The electron (COD) balances closed with a recovery of 105 % and 93 % for reactor conditions with 10 and 20 g/L NaCl concentration, respectively. At 30 g/L NaCl, only 58 % of the glycerol was converted into propionate during the anaerobic phase, leading to the observed accumulation of propionate. The remaining glycerol and the formed propionate were subsequently oxidized during the aerobic phase. In seawater conditions, complete anaerobic glycerol uptake and PHV formation were observed. The COD balance closed with a recovery of 110 % and the EBPR process was restored.

3.4. Osmotic shock test

To assess the effect of hypoosmotic conditions on biomass activity, batch tests were performed with biomass taken from the reactor at the end of the aerobic phase and placed in demineralized water sparged with nitrogen. No trehalose was detected in the bulk liquid during the normal cycles of reactor operation. Demineralized water was used to minimise the presence of cations and anions. Liquid samples were taken and analysed by an HPLC and the results are shown in Fig. 5.

Incubation of salt-adapted granules in demineralized water showed significant trehalose and accompanied phosphate release (Table 5). The maximum release occurred rapidly within minutes and then reached a plateau (Fig. 5).

Table 4
List of anaerobic rates and stoichiometries. P_{rel}: Phosphorus release, PHA_{pro}: PHA production, C_{up}: Carbon uptake, Gly_{deg}: Glycogen degradation. * Values from the freshwater conditions are retrieved from (Elahinik et al., 2022) and are provided as a reference. ** indicates estimated values which are calculated based on the PHA accumulated.

Salt	Freshwater*	NaCl 10	NaCl 20	NaCl 30	Sea salt 35	*g/L*
Stoichiometries						
P_{rel}/C_{up}	0.23	0.15	0.16	0.00	0.28	*Pmol/Cmol*
PHA_{up}/C_{up}	0.97	1.98	1.66	0.85	2.66	*Cmol/Cmol*
Gly_{deg}/C_{up}**	0.27	0.87	0.98	0.46	1.65	*Cmol/Cmol*
Rates						
qS	2.0	1.0	1.5	0.2	0.7	*Cmmol/gVSS/h*
qP_{rel}	11.3	2.3	6.0	0.1	6.1	*mgP/gVSS/h*
qP_{up}	16.3	7.9	11.8	0.0	3.6	*mgP/gVSS/h*

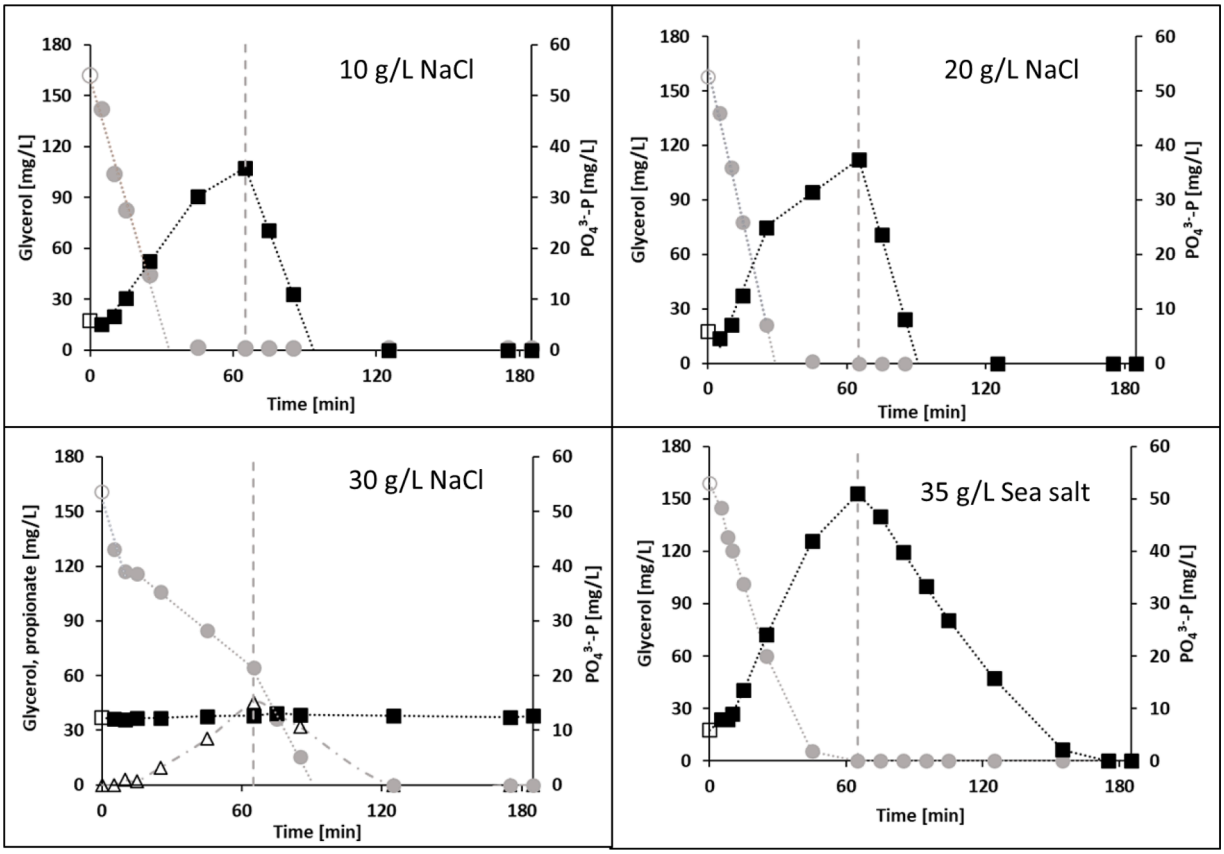

Fig. 4. Glycerol (circles), and PO_4^{3-}-P (squares) profiles during a typical cycle at each salt concentration. Propionate (triangles) accumulation is shown at 30 g/L NaCl. The dashed vertical lines indicate the switch between anaerobic and aerobic phases. The hollow points at time 0 are calculated concentrations based on influent concentration and the dilution.

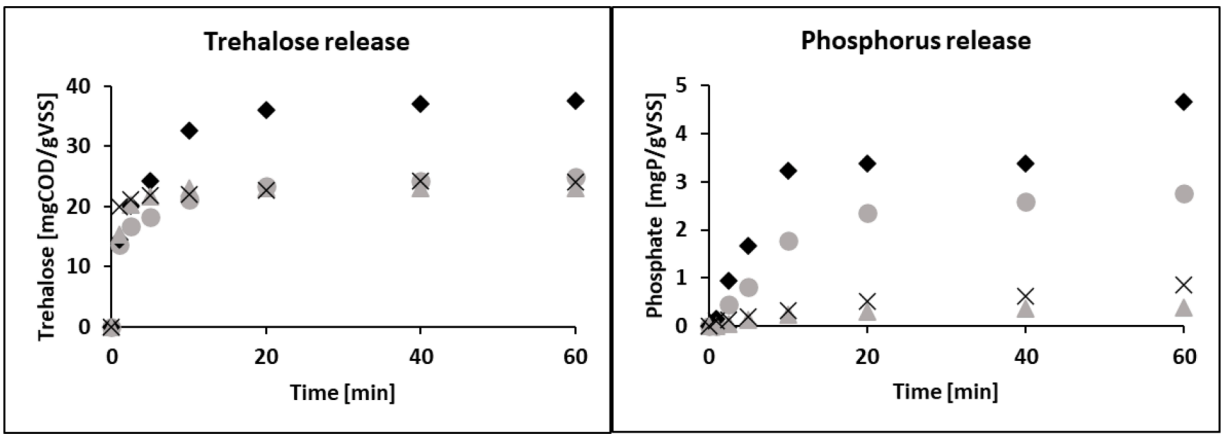

Fig. 5. Trehalose and phosphate release as a function of time under anaerobic conditions. Biomass cultivated in 10 g/L NaCl (circles), 20 g/L NaCl (diamonds), 30 g/L NaCl (triangles), and 35 g/L sea salt (crosses).

Table 5
List of trehalose and orthophosphate release of the biomass cultivated in 10–30 g/L NaCl and 35 g/L sea salt.

Parameters	Values				Units
Salt concentration	10 g/L NaCl	20 g/L NaCl	30 g/L NaCl	35 g/L Seasalt	*g/L*
Trehalose release	20.9	32.2	20.6	21.6	*mg/gVSS*
PO_4^{-3}-P release	2.4	3.4	0.2	0.9	*mg/gVSS*

3.5. Microbial community

To visually observe the changes in the microbial community distribution, frequent microscopic analysis was performed. At 10 and 20 g/L NaCl, the microbial community looked similar to the microbial community of a fresh-water system, where two morphologically distinct microorganisms were present (Fig. 6.A). The microbial community structure of a fresh-water AGS system with glycerol as the carbon source is described in Elahinik et al. (2022). The first group consisted of cocci with white storage material indicating a probable presence of *Ca.* Accumulibacter, a common PAO found in EBPR systems. Meanwhile, the second group exhibited cocci arranged in tetrads, suggesting the likely presence of *Tessaracoccus,* a fermentative glycogen-accumulating organism (fGAO), capable of anaerobic glycerol conversion. At 30 g/L NaCl, while tetrad-like microorganisms were detected, the PAOs could not be detected. Notably, the tetrad-like organisms were not detected at 35 g/L sea salt and large circular cells were observed instead.

To further evaluate the microbial community of the reactor conditions of each salinity, biomass samples from the end of each condition were used for metagenome sequencing. The metagenome data was only used as a constructed dataset for the metaproteome analysis. Metaproteomics were performed in parallel to track the potential changes of protein expression with respect to different salinities as well as estimation of the microbial community distribution based on protein mass fraction. The relative abundance of the top 5 genera in each reactor is shown in Fig. 7. The fraction labelled as “other” are known but low

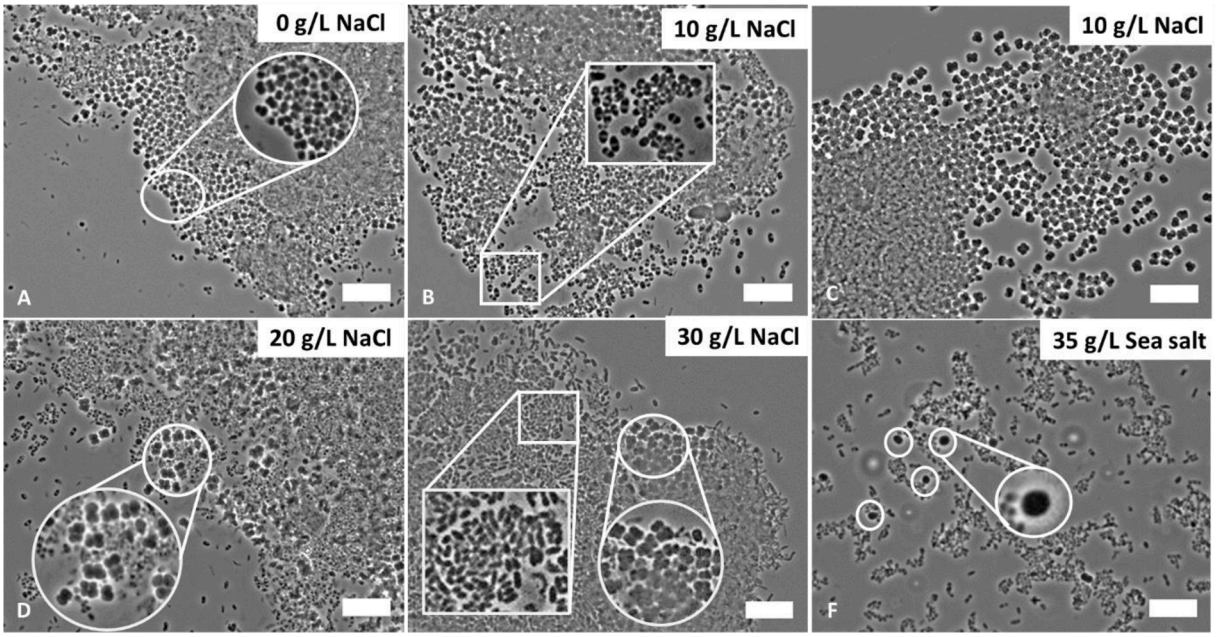

Fig. 6. Phase contrast images of the microbial community representing each condition. Square delineations show the hoarder population, i.e. PAOs, and circle delineations show the fermentative population, likely responsible for the conversion of glycerol. Picture A shows the microbial community of the reactor in fresh-water conditions as a reference. Picture C shows a cluster of tetrad microorganisms. Pictures B, D, E, & F show the microbial community of each respective salinity.

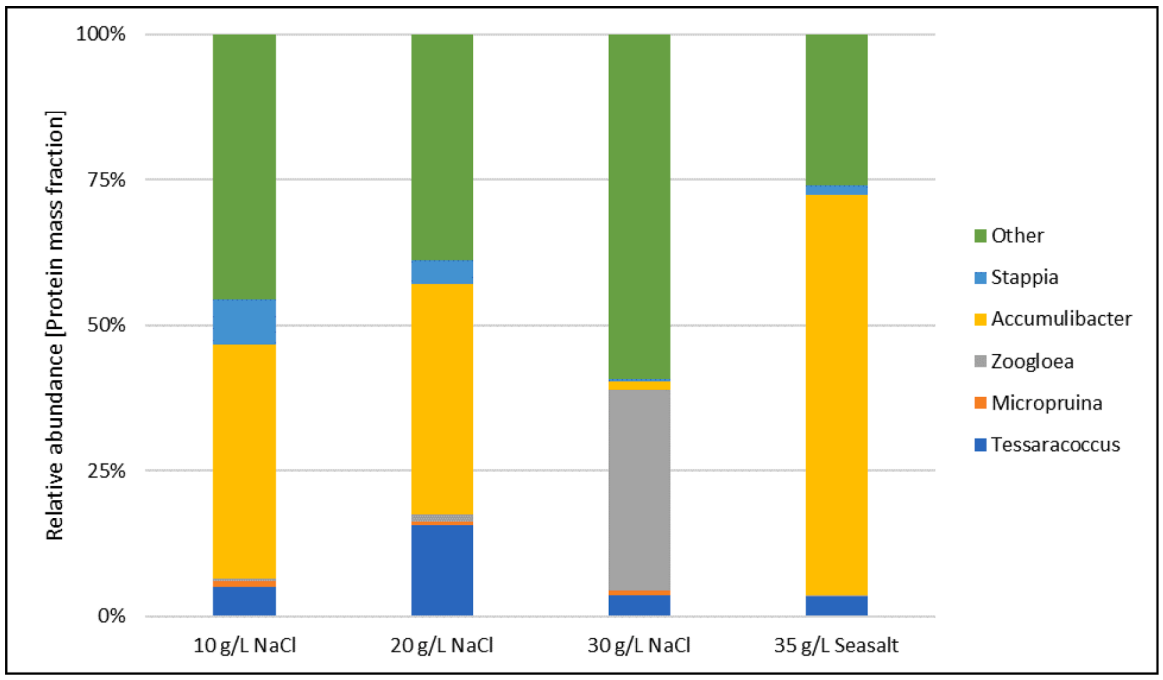

Fig. 7. The relative abundance of the top 5 genera across the reactor conditions with respective salinities based on protein mass fraction.

abundant taxa with very low protein masses and thus are not assigned. In reactor conditions exhibiting stable granulation and efficient EBPR performance, *Ca.* Accumulibacter emerged as the predominant microorganism. At 30 g/L NaCl, where both EBPR efficiency and granulation deteriorated, *Zoogloea* outcompeted *Ca.* Accumulibacter, establishing itself as the dominant taxon. Throughout all reactor conditions, *Tessaracoccus* and *Micropruina*, both actinobacteria, persisted, albeit with a low relative abundance. Similarly, *Stappia*, a motile, Gram-negative aerobe, also maintained a presence across all reactor conditions.

The key protein expressions involved in trehalose, polymer storage, polyphosphate, glycerol, potassium, and magnesium metabolism in PAOs (*Ca.* Accumulibacter) and fGAOs (actinobacteria), the two dominant taxa in stable reactor conditions, are listed in Table 6. Note that the absence of indicated proteins does not necessarily imply their non-existence within the microorganism as it may be attributed to the limitations of detection methods and extraction protocol.

Table 6
List of key metabolisms and respective proteins in PAOs and fGAOs as dominant taxa across all reactor conditions with stable operation.

Metabolisms	Proteins	Symbols	PAOs	fGAOs
Trehalose	α,α-trehalase	*TreA*	–	–
	1-α-D-glucosylmutase	*TreY/glgY*	+	–
	Isoamylase	*TreX*	+	–
	Trehalohydrolase	*TreZ/glgZ*	+	–
Storage polymer	1,4-α-glucan branching enzyme	*glgB*	–	+
	Glucose-1-phosphate adenylyltransferase	*glgC*	+	–
	Starch synthase	*glgE*	–	–
	α-maltose-1-phosphate synthase	*glgM*	+	+
	Glycogen phosphorylase	*glgP*	–	+
	PHA synthase	*phaC*	+	–
	PHA polymerase	*phaE*	+	–
	Acetoacetyl-CoA reductase	*phbB*	+	+
	Acetyl-CoA synthetase	*acs*	+	+
	Propionyl-CoA synthetase	*prpE*	+	–
Polyphosphate	Phosphotransferase	*pap*	+	–
	Exopolyphosphatase	*ppx*	+	–
	Polyphosphate glucokinase	*ppgk*	+	–
	Polyphosphate kinase	*ppk*	+	–
Glycerol	Glycerol-3-phosphate dehydrogenase	*glpA/B/C/D*	–	+
	Glycerol uptake facilitator	*glpF*	–	+
	Glycerol kinase	*glpk*	–	+
Potassium	K^+ uptake protein	*trkA*	+	+
	K^+-dependent mechanosensitive channel	*kefA/aefA*	+	–
Magnesium	Mg^{2+} exporter	*tlyC*	+	–
	Mg^{2+} transporter	*corA*	+	–

4. Discussion

An AGS reactor was operated in SBR mode to investigate and compare the effect of various concentrations of NaCl and synthetic seawater on granulation, anaerobic-aerobic conversions, phosphate removal, and changes in the microbial community. Glycerol was used as the carbon source since it is regularly present in industrial wastewaters and to allow the evaluation of microbial interactions that better reflect real conditions. The results showed that granulation and phosphate removal deteriorated with 30 g/L NaCl while at similar NaCl concentrations but under seawater conditions, the reactor operation behaved comparable to fresh-water conditions. The findings and the potential underlying mechanisms are discussed.

4.1. Influence of ionic property differences on AGS and EBPR

Phosphate removal was affected by increasing NaCl concentration, particularly at 30 g/L (Fig. 1). Both anaerobic P-release and aerobic P-uptake gradually decreased until no more release or uptake was observed. Several reasons for EBPR failure at elevated salt concentrations have been reported in the literature, such as inhibition of PAOs due to nitrite accumulation (Pronk et al., 2014), out competition of PAOs by GAOs (Bassin et al., 2011), enrichment of different type of PAOs with PAO clade I being more tolerant than PAO clade II to salt stress (Z. Wang et al., 2018), or shift of energy generation from poly-P dependent ATP generation to energy generation via glycolysis (Welles et al., 2014). In this study, phosphate removal was restored when synthetic seawater was used instead of NaCl. Using synthetic seawater, de Graaff et al. (2020a) also showed stable granulation and phosphate removal with comparable operation to freshwater AGS systems. The reactor with

synthetic seawater contained similar concentrations of NaCl as the reactor with 30 g/L NaCl, yet both reactor conditions manifested a different operational performance. Since other operational parameters were kept constant, we postulate that it is the ionic property of the medium (i.e. the ratio of cations) that affects EBPR in saline environments. The additional salts present in seawater, such as Mg^{2+} and K^{+}, appear to counteract the negative effects of Na^{+} on cellular activity. Transport of Na^{+} and K^{+}across the cell membrane plays an important role in several cellular homeostatic mechanisms including osmoregulation (Kakinuma and Harold, 1985). The primary response to increased osmolarity in both Gram-negative and -positive microorganisms is characterized by the quick uptake of potassium ions to neutralize the negative charges on halophilic enzymes (Sleator and Hill, 2001). This neutralization process serves to counterbalance the repulsive forces on the enzymes and prevent protein denaturation during osmotic fluctuations. Potassium is also reported to play an important role in the water activity of the cell, and the ability of some non-halophilic organisms to tolerate high salt concentrations is closely linked to their capacity to accumulate K^{+} (Christian and Waltho, 1961). In a study involving 32 strains of both Gram-negative and -positive microorganisms, an inverse relationship was observed between cellular K^{+} and Na^{+} content. This finding suggests that organisms with a higher K^{+} content, which is often associated with greater salt tolerance, tend to have a lower Na^{+} concentration (Christian and Waltho, 1961). The Na^{+}-K^{+} pump works by exporting 3 Na^{+}ions and importing 2 K^{+}ions into the cell which could be interrupted by the high Na^{+}/K^{+}ratio in the medium. The addition of salts, such as Mg^{2+} and K^{+}, as a strategy to enhance the biological treatment of organically polluted brines has only received limited attention in the current literature until recently. For instance, studying the anaerobic digestion of an organically polluted brine, Li et al. (2018) found that the addition of potassium salt increased the process's efficiency in terms of COD removal. The authors also reported stimulated dehydrogenase activities and maintenance of the morphology of anaerobic microorganisms at a higher K^{+}/Na^{+}ratio. Moreover, Sudmalis et al. (2018), in their examination of osmolytes and their potential to alleviate osmotic stress in anaerobic granular sludge systems, observed that the introduction of potassium (relative to sodium) at a ratio equivalent to seawater (27 w/w - Table 1) could alleviate the osmotic stress experienced by methanogens during the incubation period. For PAOs in particular, $K^{+}$is also an essential element since it is taken up aerobically (along with Mg^{2+}or Ca^{2+}) as a counter ion to PO_4^{3-} (van Groenestijn et al., 1988) and thus, lack or insufficient amount of necessary cations in the medium interrupts their activity. Considering the above discussion, the significantly higher Na^{+}/K^{+} and Na^{+}/Mg^{2+}in the reactor with 30 g/L NaCl (Table 1), could potentially be the cause of disruption in microbial processes, including phosphate uptake.

4.2. Microbial community dynamics as a function of salinity

A previous study highlighted the intricate process of glycerol conversion in an AGS-EBPR system which involved the combination of substrate fermentation by members of the actinobacteria such as *Tessaracoccous* and *Micropruina* (i.e. fGAO) and product uptake by *Ca.* Accumulibacter (i.e. PAO) (Elahinik et al., 2022). In this study, these microorganisms were also present in the system even at elevated salinities. The fGAOs possess the enzymatic machinery to convert sugars into fatty acids which can be assimilated by the PAOs into PHA under anaerobic conditions. It was shown that glycerol is mainly fermented into propionate by the fGAOs and propionate is taken up by the PAOs. With the assumption that glycerol conversion to propionate was done solely by the fGAOs, it can indicate that these organisms are not inhibited at 30 g/L NaCl since propionate accumulation was observed, although their metabolic rates decreased significantly (Fig. 4). PAOs on the other hand are completely inhibited at 30 g/L NaCl since both phosphate and propionate uptake were halted. As a consequence of substrate overflow into the aerobic phase, the genus *Zoogloea*, a notorious microorganism known for its excessive extracellular polymeric substance (EPS) production and floc formation replaced PAOs as the dominant taxon. These microorganisms are Gram-negative, facultative aerobes that can utilize a wide range of substrates (Shao et al., 2009). The proliferation of *Zoogloea* in WWTPs has been linked to sludge bulking, scum formation, and increased effluent turbidity (Novak et al., 1994), phenomena that were also observed in the reactor at 30 g/L NaCl. In full-scale granular sludge reactors, the occurrence of *Zoogloea* is observed to be related to insufficient readily biodegradable COD removal under anaerobic feeding conditions.

The absence of glycerol metabolizing enzymes in PAOs was used to indicate their inability to directly utilize glycerol (Elahinik et al., 2022). The batch tests (Fig. 3) and the metaproteome analysis in this study support the genome-based evaluation. As expected, PAOs possess the proteins involved in polyphosphate, PHA, and glycogen metabolism. The proteins involved in trehalose metabolism such as *TreY, TreX*, and *TreZ* were also detected in PAOs. The presence of genes encoding for *TreA, TreY, TreX, and TreZ* in the genome *Ca.* Accumulibacter was previously reported by de Graaff et al. (2021). In short, *TreY* (glucosylmutase) catalyses the conversion between different forms of glucose linkages within a molecule, *TreX* (isoamylase) breaks down glycogen molecules for energy production during periods of increased energy demand, and *TreZ* (trehalase) catalyses the breakdown of trehalose into glucose molecules, a requirement for ATP production. Interestingly, none of these enzymes was found in fGAOs. This lack of detection could be either due to extraction bias or an indication that these microorganisms might have a different coping mechanism for osmotic stress. Moreover, proteins involved in both potassium and magnesium transport across the cellular membrane, essential for osmoregulation and metabolising polyphosphate, were all detected in PAOs. The lack of *PhaC* and polyphosphate metabolising enzymes in the fGAOs subject to this study confirms the previous findings that they do not contribute to PHA accumulation and phosphate removal in EBPR systems (Elahinik et al., 2022, 2023).

4.3. Cytoplasmic solute and osmoregulation

Transfer of salt-adapted enrichment to demineralized water resulted in a rapid trehalose release (Fig. 5). Trehalose is a disaccharide, compatible solute accumulated in microorganisms as a response to stress conditions. One of the stress management strategies bacterial species have developed is the ability to accumulate compatible solutes which helps in cell rehydration without interfering with cellular activity (Ruhal et al., 2013). Just like their ability to accumulate, microorganisms have also developed a mechanism in which they can rapidly eject the compatible solutes to regulate their turgor pressure (hydrostatic pressure between the cell interior and exterior) when transitioning from environments of high to low osmolarity (Sleator and Hill, 2001). The biosynthesis of trehalose in bacteria is proposed to follow different pathways depending on the carbon source and the microorganism (Ruhal et al., 2013). Different sugars such as glucose and glycerol for trehalose production have been studied and the metabolic pathways for trehalose biosynthesis in different microorganisms are extensively described in the literature (Cardoso et al., 2004; Dalmasso et al., 2012; Giaever et al., 1988; Ruhal and Choudhury, 2012; Wu et al., 2017). However, information on trehalose transformations in the context of wastewater ecology is scarce although it is a metabolite that plays an important role in saline conditions. In a previous study, trehalose was identified as an osmoprotectant in *Ca.* Accumulibacter, pointing out the metabolic flexibility and the coping mechanism of these microorganisms to salinity (de Graaff et al., 2021). In this study, during the batch test, in addition to the release of trehalose, a considerable amount of P-release was also observed (Fig. 5). This observation suggests that the ejection of trehalose, which is necessary for osmoregulation, phosphate, and potentially other compounds are released due to the passive efflux of cytoplasmic solutes. Under increased membrane tension (low

osmolarity), mechanosensitive channels on the cell membrane open to allow passage of water and cytoplasmic solutes (Buda et al., 2016), including metabolites, ions, and ATP (Berrier et al., 1992; Epstein, 1986).

4.4. Effluent turbidity and granule morphology at elevated NaCl concentration

Compact granular sludge with a low SVI_5 of <20 mL/g was achieved at all tested salinities. The formation of granules shows that granulation is not hampered due to salt presence. Increasing NaCl concentration resulted in higher effluent turbidity and altered the morphology of the granules. It is a common observation that effluent turbidity increases at elevated NaCl concentrations (Bassin et al., 2011). At 33 g/L NaCl, Pronk et al. (2014) reported a washout of single-cell bacteria encapsulated in acidic polysaccharides, a constituent of the EPS, via the effluent. They hypothesized that the weakening of the EPS and detachment of granules (hence higher effluent turbidity) at higher NaCl concentrations might be due to the replacement of Ca^{2+}ions by Na^{+}. However, these arguments explaining the underlying mechanisms are speculative and thus require further research. In this study, at 30 g/L NaCl, the change in the microbial community (proliferation of genus *Zoogloea*) likely due to aerobic availability of rbCOD can explain the increase in effluent turbidity. Haaksman et al. (2020) studied the effect of incomplete anaerobic substrate uptake on the morphology and process stability of the AGS systems. It was shown that the aerobic conversion of minor amounts of rbCOD, by granules enriched for anaerobic storage, results in minor filamentous growth on the granule's surface. This phenomenon was observed in the reactor condition with 30 g/L NaCl (Fig. 2.C) where substrate overflow to the aerobic phase occurred (Fig. 4). Switching from NaCl to seawater condition, smooth granules were restored (Fig. 2. E) and the effluent suspended solid concentration decreased by three folds to approximately 100 mg/L (Table 3) which is comparable to the concentration of about 70 mg/L in freshwater conditions with glycerol as substrate (Elahinik et al., 2022). These values are slightly higher than the concentration of 20 mg/L reported from a similar system (AGS operated in synthetic seawater) running on acetate as substrate (de Graaff et al., 2020a). Since the effluent turbidity was higher in both fresh and seawater conditions with glycerol compared to acetate as substrate, it can indicate that effluent turbidity is likely to be affected by other factors such as the substrate and not necessarily by the salinity. An effluent TSS of 90 mg/L was also observed in a fresh-water reactor fed with glucose as substrate (Elahinik et al., 2023), which raises the question of whether using sugars as substrate can lead to a more turbid effluent compared to VFAs such as acetate or propionate. A possible explanation for higher effluent turbidity with sugars could be the different microbial communities, forming an EPS with different properties.

4.5. Practical implications

- In wastewater treatment processes for saline streams, the ratios of cations may play a more significant role than the absolute concentrations. The ionic properties of the influent can affect not only phosphate removal but also the effluent quality in terms of solids concentration. Therefore, it is crucial to consider not only the total salinity but also the ratio of cations for an effective treatment. This can be achieved through mixing the influent with seawater if available or adjusting the ratios of cations in the wastewater influent by the addition of salts. Therefore, identification of the minimum ratio of major cations such as Mg2+, Ca2+, and K+ relative to Na+ required for a stable AGS system could help alleviate the limitations of saline wastewater treatment biologically.
- Effluent turbidity can be a concern in full-scale applications but is often neglected in scientific literature. Fluctuating salt concentrations in the influent of WWTPs interrupt the metabolic activity of microorganisms, causing the discharge of cellular molecules such as trehalose that would negatively affect the effluent quality. Moreover, the elevated salt concentrations change the microbial community which in turn affects the effluent quality such as increased turbidity. Maintaining a reactor with a stable microbial population proves effective in treating saline streams and minimizing effluent turbidity.
- Overflow of biodegradable COD to the aerated phase leads to the filamentous growth of heterotrophs in AGS systems such as *Zoogloea* and ultimately causes sludge bulking. Therefore the detection of *Zoogloea* might be a good biomarker for systems with suboptimal operation of the anaerobic phase.
- Research endeavours about the impact of salt require special consideration of experimental procedures due to the interference of high salinity with analytical techniques.

5. Conclusion

- Successful granulation and long-term stable reactor operation were shown at 10 and 20 g/L NaCl and seawater condition (35 g/L) using glycerol as the carbon source.
- Incomplete anaerobic substrate uptake at 30 g/L NaCl led to aerobic conversions. This led to filamentous growth and gradual deterioration of granular structure.
- *Ca.* Accumulibacter was the dominant taxon in stable AGS reactors performing EBPR at 10 and 20 g/L NaCl and seawater conditions (35 g/L).
- In the reactor condition with 30 g/L NaCl, characterized by impaired granulation and turbid effluent, *Zoogloea* emerged as the predominant taxon.
- Cellular compounds including trehalose and PO_4^{3-}-P were released from salt-adapted biomass during osmotic down shock.
- The ionic composition of wastewater is likely to be more important for the AGS reactor's operational stability and EBPR than absolute salt concentration.

Declaration of AI-assisted technologies in scientific writing

During the preparation of this work, the author used ChatGPT 3.5 in order to improve the structure and readability of some sentences. After using this tool, the author reviewed and edited the content as needed and takes full responsibility for the content of the publication.

CRediT authorship contribution statement

Ali Elahinik: Writing – original draft, Visualization, Methodology, Investigation, Formal analysis, Data curation, Conceptualization. **Fleur de Clercq:** Investigation. **Martin Pabst:** Methodology, Investigation. **Dimitrios Xevgenos:** Funding acquisition. **Mark C.M. van Loosdrecht:** Writing – review & editing, Supervision, Methodology, Conceptualization. **Mario Pronk:** Writing – review & editing, Supervision, Methodology, Conceptualization.

Declaration of competing interest

The authors declare that they have no known competing financial interests or personal relationships that could have appeared to influence the work reported in this paper.

Data availability

Data will be made available on request.

Acknowledgement

This project was funded by WATER-MINING which is a research and

innovation project that develops energy-efficient technologies for treating municipal and industrial wastewaters, whilst promoting resource recovery. WATER-MINING (Grant Agreement No 869474) is partially funded by the European Union Horizon 2020 research and innovation programme. For further information regarding the project, the reader can refer to https://watermining.eu/.

References

Atkinson, M.J., Bingman, C., Box, P.O., Bingman, C., Box, P.O., 1997. Elemental composition of commercial seasalts. J. Aquaricult. Aquatic Sci. (2), 39–43. *VIII*.

Barnard, J.L., 1975. Biological nutrient removal without the addition of chemicals. Water Res. 9 (5–6), 485–490. https://doi.org/10.1016/0043-1354(75)90072-X.

Bassin, J.P., Kleerebezem, R., Dezotti, M., van Loosdrecht, M.C.M., 2012. Simultaneous nitrogen and phosphate removal in aerobic granular sludge reactors operated at different temperatures. Water Res. 46 (12), 3805–3816. https://doi.org/10.1016/j.watres.2012.04.015.

Bassin, J.P., Pronk, M., Muyzer, G., Kleerebezem, R., Dezotti, M., van Loosdrecht, M.C.M., 2011. Effect of elevated salt concentrations on the aerobic granular sludge process: linking microbial activity with microbial community structure. Appl. Environ. Microbiol. 77 (22), 7942–7953. https://doi.org/10.1128/AEM.05016-11.

Bengtsson, S., de Blois, M., Wilén, B.M., Gustavsson, D., 2018. Treatment of municipal wastewater with aerobic granular sludge. Crit. Rev. Environ. Sci. Technol. 48 (2), 119–166. https://doi.org/10.1080/10643389.2018.1439653.

Berrier, C., Coulombe, A., Szabo, I., Zoratti, M., Ghazi, A., 1992. Gadolinium ion inhibits loss of metabolites induced by osmotic shock and large stretch-activated channels in bacteria. Eur. J. Biochem. 206 (2), 559–565. https://doi.org/10.1111/j.1432-1033.1992.tb16960.x.

Beun, J.J., Hendriks, A., Van Loosdrecht, M.C.M., Morgenroth, E., Wilderer, P.A., Heijnen, J.J., 1999. Aerobic granulation in a sequencing batch reactor. Water Res. 33 (10), 2283–2290. https://doi.org/10.1016/S0043-1354(98)00463-1.

Buda, R., Liu, Y., Yang, J., Hegde, S., Stevenson, K., Bai, F., Pilizota, T., 2016. Dynamics of Escherichia coli's passive response to a sudden decrease in external osmolarity. Proc. Natl. Acad. Sci. U.S.A. 113 (40), E5838–E5846. https://doi.org/10.1073/PNAS.1522185113.

Cardoso, F.S., Gaspar, P., Hugenholtz, J., Ramos, A., Santos, H., 2004. Enhancement of trehalose production in dairy propionibacteria through manipulation of environmental conditions. Int. J. Food Microbiol. 91 (2), 195–204. https://doi.org/10.1016/S0168-1605(03)00387-8.

Christian, J.H., Waltho, J.A., 1961. The sodium and potassium content of non-halophilic bacteria in relation to salt tolerance. J. Gen. Microbiol. 25 (1), 97–102. https://doi.org/10.1099/00221287-25-1-97.

Dalmasso, M., Aubert, J., Even, S., Falentin, H., Maillard, M.B., Parayre, S., Loux, V., Tanskanen, J., Thierry, A., 2012. Accumulation of Intracellular Glycogen and Trehalose by Propionibacterium freudenreichii under conditions mimicking cheese ripening in the cold. Appl. Environ. Microbiol. 78 (17), 6357–6364. https://doi.org/10.1128/AEM.00561-12.

de Bruin, L.M.M., de Kreuk, M.K., van der Roest, H.F.R., Uijterlinde, C., van Loosdrecht, M.C.M., 2004. Aerobic granular sludge technology: an alternative to activated sludge? Water Sci. Techn. 49 (11–12), 1–7. https://doi.org/10.2166/wst.2004.0790.

de Graaff, D.R., van Loosdrecht, M.C.M., Pronk, M., 2020a. Biological phosphorus removal in seawater-adapted aerobic granular sludge. Water Res. 172, 115531 https://doi.org/10.1016/j.watres.2020.115531.

de Graaff, D.R., van Loosdrecht, M.C.M., Pronk, M., 2020b. Stable granulation of seawater-adapted aerobic granular sludge with filamentous Thiothrix bacteria. Water Res. 175, 115683 https://doi.org/10.1016/j.watres.2020.115683.

de Graaff, D.R., van Loosdrecht, M.C.M., Pronk, M., 2021. Trehalose as an osmolyte in Candidatus Accumulibacter phosphatis. Appl. Microbiol. Biotechnol. 105 (1), 379–388. https://doi.org/10.1007/s00253-020-10947-8.

de Kreuk, M.K., van Loosdrecht, M.C.M., 2004. Selection of slow growing organisms as a means for improving aerobic granular sludge stability. Water Sci. Techn. 49 (11–12), 9–17. https://doi.org/10.2166/wst.2004.0792.

Elahinik, A., Haarsma, M., Abbas, B., Pabst, M., Xevgenos, D., van Loosdrecht, M.C.M., Pronk, M., 2022. Glycerol conversion by aerobic granular sludge. Water Res. 227, 119340 https://doi.org/10.1016/J.WATRES.2022.119340.

Elahinik, A., Li, L., Pabst, M., Abbas, B., Xevgenos, D., van Loosdrecht, M.C.M., Pronk, M., 2023. Aerobic granular sludge phosphate removal using glucose. Water Res. 247, 120776 https://doi.org/10.1016/J.WATRES.2023.120776.

Epstein, W., 1986. Osmoregulation by potassium transport in Escherichia coli. FEMS Microbiol. Lett. 39 (1–2), 73–78. https://doi.org/10.1016/0378-1097(86)90063-7.

EU Water Framework Directive. (2000). *EU water framework directive*.

Figueroa, M., Mosquera-Corral, A., Campos, J.L., Méndez, R., 2008. Treatment of saline wastewater in SBR aerobic granular reactors. Water Sci. Techn. 58 (2), 479–485. https://doi.org/10.2166/wst.2008.406.

Giaever, H.M., Styrvold, O.B., Kaasen, I., Strøm, A.R., 1988. Biochemical and genetic characterization of osmoregulatory trehalose synthesis in Escherichia coli. J. Bacteriol. 170 (6), 2841–2849. https://doi.org/10.1128/jb.170.6.2841-2849.1988.

Haaksman, V.A., Mirghorayshi, M., van Loosdrecht, M.C.M., Pronk, M., 2020. Impact of aerobic availability of readily biodegradable COD on morphological stability of aerobic granular sludge. Water Res. 187, 116402 https://doi.org/10.1016/j.watres.2020.116402. September.

Haaksman, V.A., Schouteren, M., van Loosdrecht, M.C.M., Pronk, M., 2023. Impact of the anaerobic feeding mode on substrate distribution in aerobic granular sludge. Water Res. 233, 119803 https://doi.org/10.1016/J.WATRES.2023.119803.

Heijnen, J.J., Van Loosdrecht, M.C.M., 1998. Method for acquiring grain-shaped growth of a microorganism in a reactor. Biofutur. European Patent Office. https://doi.org/10.1016/s0294-3506(98)80325-6.

Kakinuma, Y., Harold, F.M., 1985. ATP-driven exchange of Na+ and K+ ions by Streptococcus faecalis. J. Biological Chem. 260 (4), 2086–2091. https://doi.org/10.1016/S0021-9258(18)89520-5.

Lefebvre, O., Moletta, R., 2006. Treatment of organic pollution in industrial saline wastewater: a literature review. Water Res. 40 (20), 3671–3682. https://doi.org/10.1016/J.WATRES.2006.08.027.

Li, J., Shi, W., Jiang, C., Bai, L., Wang, T., Yu, J., Ruan, W., 2018. Evaluation of potassium as promoter on anaerobic digestion of saline organic wastewater. Bioresour. Technol. 266, 68–74. https://doi.org/10.1016/J.BIORTECH.2018.06.066.

Madigan, Martinko, J.M., Parker, J, 2000. Brock biology of microorganisms, 11. Prentice hall, Upper Saddle River, NJ.

Morgenroth, E., Sherden, T., Van Loosdrecht, M.C.M., Heijnen, J.J., Wilderer, P.A., 1997. Aerobic granular sludge in a sequencing batch reactor. Water Res. 31 (12), 3191–3194. https://doi.org/10.1016/S0043-1354(97)00216-9.

Novak, L., Larrea, L., Wanner, J., Garcia-Heras, J.L., 1994. Non-filamentous activated sludge bulking caused by Zoogloea. Water Sci. Techn. 29 (7), 301–304. https://doi.org/10.2166/WST.1994.0355.

Pronk, M., Bassin, J.P., de Kreuk, M.K., Kleerebezem, R., Van Loosdrecht, M.C.M., 2014. Evaluating the main and side effects of high salinity on aerobic granular sludge. Appl. Microbiol. Biotechnol. 98 (3), 1339–1348. https://doi.org/10.1007/s00253-013-4912-z.

Pronk, M., de Kreuk, M.K., de Bruin, B., Kamminga, P., Kleerebezem, R., van Loosdrecht, M.C.M., 2015. Full scale performance of the aerobic granular sludge process for sewage treatment. Water Res. 84, 207–217. https://doi.org/10.1016/j.watres.2015.07.011.

Ruhal, R., Choudhury, B., 2012. Use of an osmotically sensitive mutant of Propionibacterium freudenreichii subspp. shermanii for the simultaneous productions of organic acids and trehalose from biodiesel waste based crude glycerol. Bioresour. Technol. 109, 131–139. https://doi.org/10.1016/j.biortech.2012.01.039.

Ruhal, R., Kataria, R., Choudhury, B., 2013. Trends in bacterial trehalose metabolism and significant nodes of metabolic pathway in the direction of trehalose accumulation. In: Microbial Biotechnology, 6. John Wiley & Sons, Ltd, pp. 493–502. https://doi.org/10.1111/1751-7915.12029.

Sanna, P., D'Addario, E., Robertiello, A., 1991. Anaerobic treatment of effluent from epoxy resins production units. Stud. Environm. Sci. 42 (C), 47–53. https://doi.org/10.1016/S0166-1116(08)70313-3.

Shao, Y., Chung, B.S., Lee, S.S., Park, W., Lee, S.S., Jeon, C.O., 2009. Zoogloea caeni sp. nov., a floc-forming bacterium isolated from activated sludge. Int. J. Syst. Evol. Microbiol. 59 (3), 526–530. https://doi.org/10.1099/IJS.0.65670-0/CITE/REFWORKS.

Sivasubramanian, R., Chen, G.hao, Mackey, H.R, 2021. Shock effects of monovalent cationic salts on seawater cultivated granular sludge. J. Hazard. Mater. 403 (July 2020), 123646 https://doi.org/10.1016/j.jhazmat.2020.123646.

Sleator, R.D., Hill, C., 2001. Bacterial osmoadaptation: the role of osmolytes in bacterial stress and virulence. FEMS Microbiol. Rev. 26 (1), 49–71. https://doi.org/10.1111/j.1574-6976.2002.tb00598.x.

Smolders, G.J.F., van der Meij, J., van Loosdrecht, M.C.M., Heijnen, J.J., 1995. A structured metabolic model for anaerobic and aerobic stoichiometry and kinetics of the biological phosphorus removal process. Biotechnol. Bioeng. 47 (3), 277–287. https://doi.org/10.1002/bit.260470302.

Sudmalis, D., Millah, S.K., Gagliano, M.C., Butré, C.I., Plugge, C.M., Rijnaarts, H.H.M., Zeeman, G., Temmink, H., 2018. The potential of osmolytes and their precursors to alleviate osmotic stress of anaerobic granular sludge. Water Res. 147 (b), 142–151. https://doi.org/10.1016/J.WATRES.2018.09.059.

van Dijk, E.J.H., Haaksman, V.A., van Loosdrecht, M.C.M., Pronk, M., 2022. On the mechanisms for aerobic granulation - model based evaluation. Water Res. 216 (November 2021), 118365 https://doi.org/10.1016/j.watres.2022.118365.

van Groenestijn, J.W., Vlekke, G.J.F.M., Anink, D.M.E., Deinema, M.H., Zehnder, A.J.B., 1988. Role of cations in accumulation and release of phosphate by acinetobacter strain 210A. Appl. Environ. Microbiol. 54 (12), 2894–2901. https://doi.org/10.1128/aem.54.12.2894-2901.1988.

Wang, X., Yang, T., Lin, B., Tang, Y., 2017. Effects of salinity on the performance, microbial community, and functional proteins in an aerobic granular sludge system. Chemosphere 184, 1241–1249. https://doi.org/10.1016/j.chemosphere.2017.06.047.

Wang, Z., Dunne, A., van Loosdrecht, M.C.M., Saikaly, P.E., 2018. Effect of salt on the metabolism of "Candidatus Accumulibacter" clade I and II. Front. Microbiol. 9 (MAR), 1–13. https://doi.org/10.3389/fmicb.2018.00479.

Welles, L., Lopez-Vazquez, C.M., Hooijmans, C.M., Van Loosdrecht, M.C.M., Brdjanovic, D., 2014. Impact of salinity on the anaerobic metabolism of phosphate-accumulating organisms (PAO) and glycogen-accumulating organisms (GAO). Appl.

Microbiol. Biotechnol. 98 (17), 7609–7622. https://doi.org/10.1007/s00253-014-5778-4.

Wu, Y., Sun, X., Lin, Y., Shen, X., Yang, Y., Jain, R., Yuan, Q., Yan, Y., 2017. Establishing a synergetic carbon utilization mechanism for non-catabolic use of glucose in microbial synthesis of trehalose. Metab. Eng. 39, 1–8. https://doi.org/10.1016/j.ymben.2016.11.001.

Xevgenos, D., Tourkodimitri, K.P., Mortou, M., Mitko, K., Sapoutzi, D., Stroutza, D., Turek, M., van Loosdrecht, M.C.M., 2024. The concept of circular water value and its role in the design and implementation of circular desalination projects. The case of coal mines in Poland. Desalination, 117501. https://doi.org/10.1016/J.DESAL.2024.117501.